Journal of Engineering and Technology

ISSN 2180-3811 eISSN 2289-814X https://journal.utem.edu.my/index.php/jet/index

STUDYING THE COLLECTOR PERFORMANCE OF UPDRAFT SOLAR CHIMNEY POWER PLANT

Walid M. A-Elmagid[1*], István Keppler[2], Ildiko Molnar[3], Mohamed F.C. Esmail[4,] and Tarek Mekhail[5]

[1]Institute of Environmental Systems,

[2]Institute of Mechanics and Machinery, Szent István University, Páter K. u. 1, Gödöllő, H-2103, Hungary.

[3]Institute of Mechatronics and Vehicle Engineering, Obuda University, Nepszinhaz Street 8, Budapest, 1081, Hungary.

[4,5] Dept. of Mech. Power Engineering, Faculty of Energy Engineering, Aswan University, Sahara City, P.O. Box: 81528, Aswan, Egypt.

* *w.abdelmaged@aswu.edu.eg*

Article history:

Received Date: 2019-11-28

Accepted Date: 2020-05-16

Keywords: Solar chimney power plant; SCPP; CFD simulations; Aswan SCPP prototype; SCPP performance

Abstract— In the shadow of increasing energy consumption, renewable energy is the best choice for a sustainable environment. The solar chimney power plant (SCPP) is a new technology; many researchers are paying their attention to improve its performance. In this study, experimental and numerical studies were used to understand the effect of the collector geometry on the SCPP performance. The SCPP prototype under our investigation is installed in Aswan city, its chimney height is 20m, its diameter is 1 m, and the collector is a square that has a side length of 28.5m. Three dimensional CFD simulations were made to calculate the temperature and velocity distribution inside two different shapes of SCPP collector. The conclusion is that the square-shaped collector achieved higher output power than the circular collector by 7.6 % at the same surface area exposed to solar radiation.

I. Introduction

Global energy consumption is proportional to the population and economic growth, which have a dramatic increase at present. In contrast, the fossil energy source suffers a decline by the time and has a harsh environmental effect. The population growth and depletion of fossil fuel sources are the main challenges in the energy production field. The most promising solution is extending the usage of renewable energy sources. Consequently, renewable energy gradually will be our primary source of energy. The solar chimney power plant is a new technology that utilizes renewable energy sources to produce electricity, for achieving its goals; it uses the combination of solar heating and chimney effect [1].

In the past, they used the solar chimney for ventilation or drying crops that comprise solar collectors and chimney. Still, recently, it is used for electricity production by installing a turbine inside a solar chimney system. Figure 1 shows the base construction of the solar chimney power plant. The operation of the SCPP carried out by a simple principle: ambient air enters peripherally to the solar collector where the air is warmed by solar radiation. The solar collector has a large transparent canopy that allows solar radiation to enter the collector. The canopy and ground of a collector make multiple diffusion and reflection of solar radiation, which increases the heat absorbed by air (works as a greenhouse).

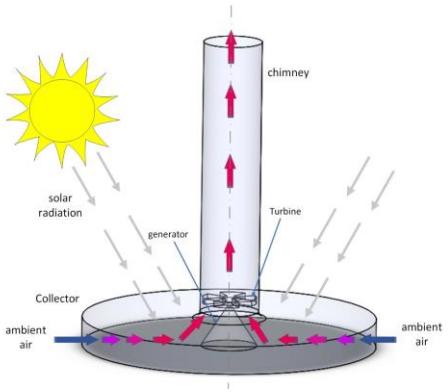

Figure 1. Schematic diagram of SCPP

The temperature difference between the bottom and top of the chimney creates the density difference that generates the driving force (buoyancy). Additionally, the change in density because of a change in altitude increases the buoyancy force.

The difference in density between the air inside the chimney and the ambient air generates a pressure potential according to the law of buoyancy that causes the flow through the solar chimney. Wind turbine, which captures most of the kinetic energy of the air can produce sufficient mechanical power. Then, it transfers the mechanical power to the generator that converts to electrical energy.

Many studies were performed using computational fluid dynamics techniques (CFD) for studying the physics phenomenon of SCPP. Muhammed et al. [2] optimized geometry construction of all the working units of SCPP by CFD software (Ansys Fluent). The validation of this analytical model is done by comparing the experimental data of Manzanares, Spain plant. Additionally, Vieira et al. [3] presented the influences of the collector inlet height and the chimney outlet diameter on the power of the device to show the applicability of the SCPP geometric optimization by studying a numerical model. Both above researchers used classical turbulence modeling (RANS) that was used for the turbulence approach with the standard k–ε model. Because of these studies, it is now possible to make a more accurate decision on consistent dimensions for a solar chimney plant using CFD software. Hassan et al. [4] used the CFD analysis of SCPP to illustrate the effects of the collector's slope and chimney divergence angle on the performance of the Manzanares prototype.

In 1981, Schwarz and Knauss designed the turbogenerator for the pilot plant in Manzanares. For this purpose, a single vertical axis turbine layout without inlet guide vanes was used [5]. On the other approach, Gannon et al. [6] proposed a single rotor with inlet guide blades approach for a large-scale turbine for solar chimney application. A three-step turbine design method, which is adapted from gas turbine literature, has been presented. Firstly, the major turbine dimensions were calculated by using a free vortex analysis method. Secondly, a matrix through flow method predicted the airflow path through the inlet guide vanes and rotor. Finally, the blade profiles were designed using an optimization code coupled to a surface vortex method to determine turbine blades of a minimum chord and low drag. The proposed turbine design can capture over 80% of the fluid power available [7],[8].

Fluri et al. [5] compared the performance of various layouts for the turbo generator proposed by the previous researchers. Furthermore, they showed that these slight changes in the modeling approach have a significant impact on performance prediction. They concluded that the lowest performances are related to the single rotor without guide vanes; the efficiency of the other three layouts is much better and lies in a narrow band. At relatively low rotational speeds, the performance of counter-rotating rotors layouts has the highest peak efficiencies, which leads to an undesirable higher torque for the same power output.

Jafarifar et al. [9] showed that strong ambient crosswinds could affect the performance of an SCPP by comparing the effect of weather conditions of the Orkney Islands in Scotland and Manzanares in Spain through numerical modeling. Their results showed that strong and steady winds could improve the performance of an SCPP. As a result, a solar chimney is a suitable option for not-too-sunny but windy weather conditions. On the other hand, Ming et al. [10] studied the effect of ambient crosswind in the performance of the SCPP. The resulting trend of the performance curve showed that external ambient crosswind has non-linearly proportional with performing SCPP that lead to optimization issue.

Kasaeian et al. [11] also studied the effect of the weather condition by testing an SCPP prototype with 10 m collector diameter and 12 m chimney height. After design and installation, measurement of the temperatures and air velocities inside the SCPP has been done. The measured results showed that the air velocity increases with increasing solar radiation on both cold and hot days from a minimum point, and after a while, it is broken by the collector warm-up. After the breaking of the increase in air velocity, a steady airflow inside the chimney would appear. Later, similar results were achieved by [12].

Making 3D simulation for the whole SCPP system has some complexity because it has many physical phenomena: rotating frame in turbine zone, radiation heat transfer in collector and heat storage in the ground. Guo et al. [13] simulated the SCPP by a three-dimensional CFD model to investigate the effects of solar radiation, turbine pressure drops, and ambient temperature on system performance and they used the turbine model. On the other hand, the whole SCPP unit with the turbine has been modeled by [14], which has the power output and the turbine efficiency of 10MW and 50%, respectively.

In this study, the 3D model of the whole SCPP with the turbine and radiation model is carried out to study velocity and temperature distribution inside collectors that have the square and circular shapes. To achieve that purpose, authors use ANSYS CFX software for solving the governing equation with the k-omega turbulence model and validate calculated results by comparing it to experimental data of the Aswan

prototype. The instantaneous temperature distribution for the solar collector at different sections is measured during a given period. Finally, the two shapes of the solar chimney collectors are compared.

II. EXPERIMENTAL PROTOTYPE

A solar chimney power plant is a unique solar plant based on the thermal conversion for electrical energy productions. Hot and dry weather is essential for the SCPP. Egypt has a significant advantage because of its hot weather and desert land availability. Egypt enjoys a solar ray for very long times that reaches 2,900 to 3,200 hours of sunshine annually with annual direct normal energy density 1, 970 to 3,200 kWh/m^2 [15], which can produce technically solar-thermal electricity-generating over 73.6 Peta-watt hour (PWh). The above weather terms encourage both the Science and Technology Development Fund (STDF) of Egypt and the Federal Ministry of Education and Research (BMBF) of Germany to establish a solar chimney power plant prototype as a jointly funded project [16].

A small-scale solar chimney, shown in Figure 2, was constructed with an inside diameter of 1 m and a height of 20 m. The chimney is manufactured from two steel tubes of a thickness of 0.8 x10^{-3} m and connected. The collector base is square of 28.5m x 28.5m side length. The collector section was opened at ground level around its outer edge by approximately 1.25 m, to allow the airflow into the system. The collector steel structure is fixed on 36 pillars set on concrete bases. The height of the pillar at the inner core is 1.5m while its height is 1.25m at the outer rim. The roof is made of a 4 x10^{-3} m thick clear glass square panels (1.48m x 1.48m) that is supported on the steel framework. The glass panels are rounded by the EPDM rubber (Ethylene Propylene Diene Monomer) for glass protection and preventing air leakage. The maximum service temperature of this rubber is 150 °C [17]. The ground surface layer was covered by sand to increase the absorption of incident solar radiation. The bottom end of the chimney was bolted on top of a steel-structured supported on a concrete base [18].

Figure 2. Aswan solar chimney power generation

The turbine of five blades is designed according to the blade element theory. The BW-3 airfoil is suitable for the low velocity of airflow for the present study. A 300-Watt generator of maglev type is coupled with the turbine hub. Figure 3(a) shows the turbine-generator unit outside the chimney, and Figure 3(b) shows the unit inside the chimney.

(a) Outside the chimney

(b) Inside the chimney

Figure 3. Turbine-Generator Unit

To obtain comprehensive data on the performance of the solar chimney system, temperature sensors were placed in three sections; one sensor is placed at the inlet of the collector at the middle of its height, three sensors were placed at the center of the collector (near the glass, at the middle and at the ground). Five temperature sensors were placed equally spaced at the exit of the collector vertically to measure the temperature distribution from the ground to underneath the glass of the collector. The laser sensor has been placed below the turbine blade to measure the rotational speed and connected wireless to the server. The temperature sensors were calibrated using thermocouples and the RPM sensor using a digital RPM measuring device. A view of these sensors is shown in Figure 4.

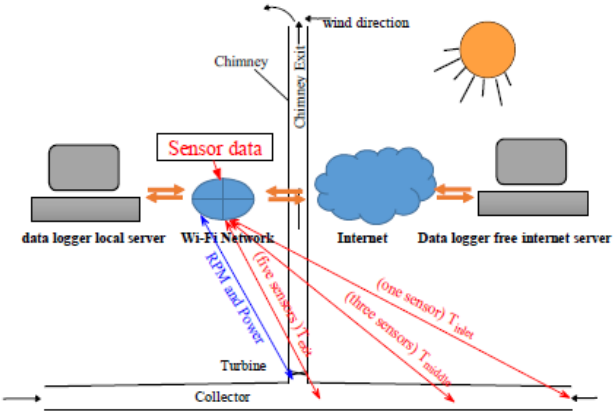

Figure 4. The schematic diagram for the whole system measurement

III. NUMERICAL MODEL

Principles of solar chimney power plants depend on many physical phenomena such as heat storage, turbomachinery, and radiation heat transfer, which increase the level of the complexity of analyzing the system. However, computational fluid dynamic (CFD) has the ability for simulation and studying the whole solar chimney system, as mentioned in the literature review section. We use ANSYS CFX version 18.1 to solve the governing equations of a solar chimney system. ANSYS CFX version 18.1 solves the conservation equation of mass, momentum, and energy with the K-omega turbulence model.

As a pre-step of the grid generation, 3D geometry of the solar chimney prototype is drawn using SOLIDWORKS version 2017 according to a prototype, which was implemented in Aswan, Egypt, as shown in Figure 5. The geometry of SCPP in Figure 5 is divided into three zones: the first zone is the fluid section that has a blue color, the second zone is the ground section that has a brown color, and the third zone is the glass cover of the collector that has a green color.

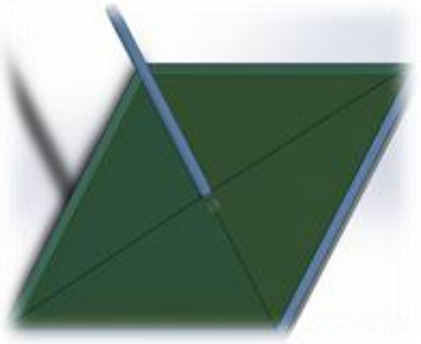

Figure 5. Three-dimension geometry of solar chimney prototype

This division process gives us the ability to use different materials domain on the ANSYS CFX model. Additionally, similar methods are applied for creating a collector having a circular shape.

Then, ANSYS Workbench Meshing software is used for creating the CFX grid for different zones of the prototype, except for the turbine domain; we used the TurboGrid program. The turbine domain needs a more beautiful network because it includes the rotating blade. The rotation of the turbine blade gives rise to the high intensity of the turbulence in the flow field.

To calculate radiation heat transfer, we use two radiation model: P-1 model solve the fluid domain and Monte Carlo model solve the solid domain as Surface-To-Surface configuration. The buoyancy phenomenon has an enormous effect on the solar chimney system, so the buoyancy model is used. The interface between the turbine domain that has the rotational motion with collector and chimney domains involve the sliding mesh. We should apply a frozen rotor model to solve this sliding mesh. The K-omega based Shear-Stress-Transport model (SST) was also used because of the treatment of the near-wall condition at low-Reynolds number computations.

One of the great features of the K-omega turbulence model is that the model does not involve the complex nonlinear damping functions required for the K-ε model and is, therefore, more accurate and more robust. A low-Reynolds K-ε model would typically require a near-wall resolution of $y < 0.2$, while a low-Reynolds number K-omega model would need at least $y < 2$. It allows for a smooth shift from a low-Reynolds number form to a wall function formulation [19].

The accuracy of the simulation model results substantially depends on the input boundary conditions. Table 1 shows the location and value of the used boundary condition in the Aswan SCP model. The height of the chimney is considered by evaluating the change of atmospheric pressure with height as well-known that the flow inside the chimney follows up a dry adiabatic lapse rate. Direct radiation and rotational of the turbine are taken from experimental data, because of continuously changing with time. The surface of the ground that contact with air-exposed to solar radiation is less than the outer cover surface by glass transmissivity. To clarify the different performance of collectors within various shapes, we use the boundary condition in Table 1 for two CFD models.

Table 1. the boundary condition of the CFD models

Location	Boundary type	Value
Inlet of collector	Opening	1 atm
Outlet of chimney	Opening	0.9967 atm (adiabatic lapse rate)
Turbine domain	Rotational farm	Rotation speed from experimental
The outer surface of the glass cover	Wall, Radiation source	Direct radiation from experimental
the surface between collector air and ground	Interface surface, a Radiation source	Direct radiation from experimental * transmissivity of glass

IV. RESULT AND DISCUSSION

A. Theoretical result

Computational fluid dynamic (CFD) is a powerful tool to analyze a physical system, so, we used ANSYS CFX software for simulation solar chimney power plant that is implemented on Aswan city. For checking the accuracy of the calculated results, we compared it with the experimental results. Figure 6 shows the vertical temperature distribution at the exit of the collector, and Figure 7 shows the vertical temperature distribution at 7.125 m (middle) of the collector. The average of the calculated result has a considerable agreement with the measured result in Figure 6 and Figure 7.

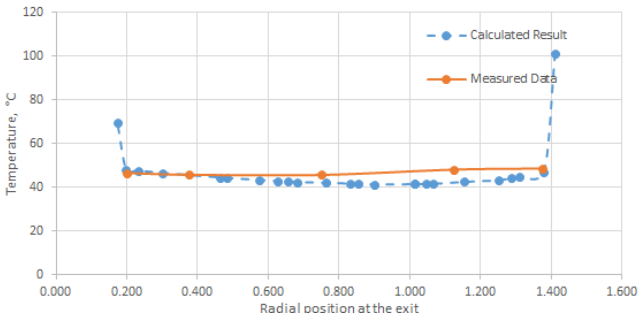

Figure 6. The temperature at the exit of the collector

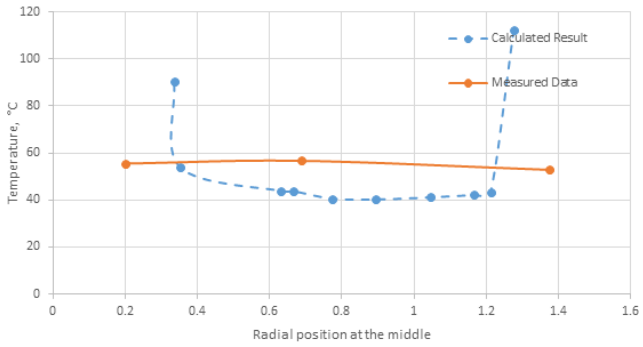

Figure 7. The temperature in the middle of the collector

As mentioned, the collector has two common shapes: circular collector and square-shaped collector, for studying the more efficient shape, we made the CFD model for both shapes. Table 2 shows the calculated results of both shapes of the collector.

Table 2. CFD results of circular and square collectors

	Circular collector	Square collector	Percentage
Geometric inlet area, m^2	151.55	171	11.4%
Effective inlet area, m^2	101.026	144.3	30%
Mass flow rate , Kg/s	13.4487	14.0507	4.3%
Outlet temperature of collector , ^0C	45.124	44.441	-1.5%
Output power , W	329.237	356.151	7.6%

The geometric calculation shows the square shape collector increases the inlet area by 11.4 % than the circular collector. The airflow isn't a uniform distribution on the inlet area because of low inlet air velocity, the reverse airflow takes place on the geometric inlet area, and the effective inlet area presents the original part of a geometric inlet area that allows the airflow inside the collector. The square collector increases the effective inlet area by approximately 30% at the same inlet height, the mass flow rate of square shape is consequently increased by 4.3 %. However, solar radiation exposed to the same surface area in both cases, but the circular shape achieves 0.683^oC higher than the square shape collector of the average exit temperature. Due to the increase in the mass flow rate, the output power that produces gains by 7.6 % based on the square calculation results.

Using a velocity vector tool in ANSYS CFX-Post, we can get more analysis of the air velocity inside the collector. Figure 8 shows the velocity vector field at height 0.65 m from the ground (approximately mid-span) and the radial direction of the velocity vector field of the square collector. Figure 8 shows the shortest radial direction from the mid-span of the square side to the center of the collector and also the longest radial direction from the corner of the square side to the center of the collector. It is different because of the different airflow path length.

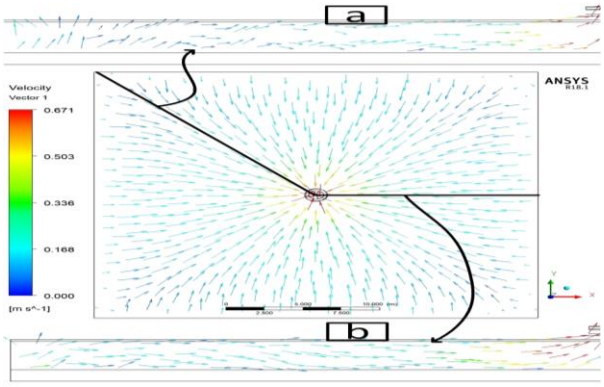

Figure 8. Velocity vector inside the square shape collector

The velocity distribution has a considerable effect on creating temperature distribution inside the collector. Figure 9 shows the temperature contour at approximately mid-span from the ground (the same plane of the velocity vector) and the radial direction of the temperature contour of the square collector.

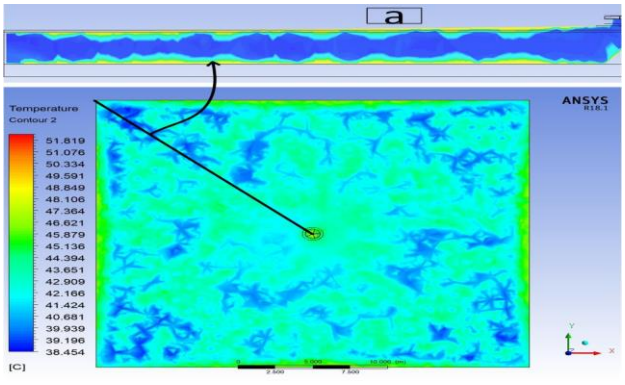

Figure 9. Temperature distribution of the square collector

For demonstrating the difference of the performance between the circular shape and square shape collectors, we follow a similar pattern of the calculated result for the circular shape collector. Figure 10 shows the velocity vector field at height 0.65 m from the ground (approximately mid-span) and the radial direction of the velocity vector field of the circular collector. The airflow suffers from high turbulence, and some reverse flow at the inlet, as shown in Figure 8 and Figure 10, both of these paths have the same length. However, the longest paths from corners to the center of the collector have more smooth airflow at the inlet area, as shown in Figure 8. Consequently, the square shape collector achieved a more substantial mass flow rate of air.

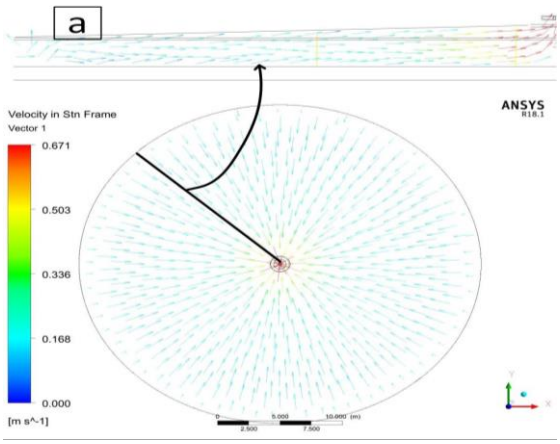

Figure 10. The velocity vector of the circular shape collector

Figure 11 shows the radial direction of the temperature contour of the circular collector and the temperature contour at approximately mid-span from the ground (the same plane of the velocity vector). The temperature distribution inside the circular shape collector is exceedingly regular, as shown in Fig 11-a. The turbulent flow assists in increasing the heat transfer by increasing the length of flow streamline and mixing processes of a laminate of the fluid. However, the square shape collector has a more turbulent flow pattern, as shown in Fig.9, it achieves less the average exit temperature of the collector by -1.6 % than the circular collector, because of the higher mass flow rate.

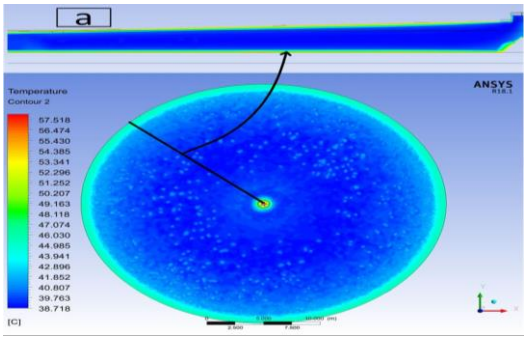

Figure 11. Temperature distribution of the circular shape collector

B. Experimental result

Heat transfer process inside the solar chimney collector carried out by combining radiation and convection heat transfers. There are five temperature sensors placed vertically and equally from the ground to the inner glass panel for showing the temperature distribution in Figure 10. The general trend of the temperature distribution shows that the ground temperature is the highest temperature among the others, and this agrees to the theoretical steady-state analysis [20].

By carefully looking at Figure 12 and some samples of the instantaneous temperature distribution at the exit of the collector at the ground (Section 1), 0.375 m from the ground (Section 2), 0.75 m from the ground (Section 3), 1.125 m from the ground (Section 4) and below the glass panels (Section 5) is selected at two different times, one at noontime and the other one at midnight.

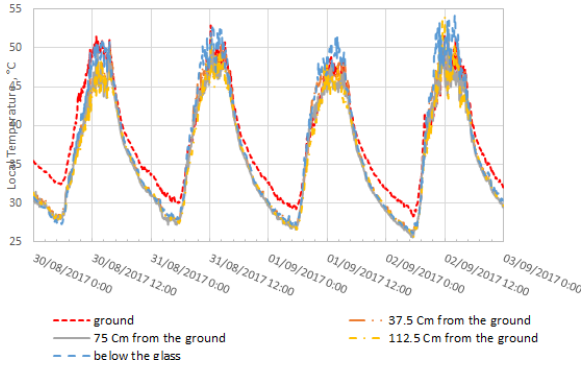

Figure 12. Transient temperature distribution at the exit plane of the collector

Figure 13 shows the maximum temperature occurs below the glass panels at noontime due to the heating of solar radiation, and it reached to 50.5 ^{0}C and decreased to 46 ^{0}.C. at the ground.

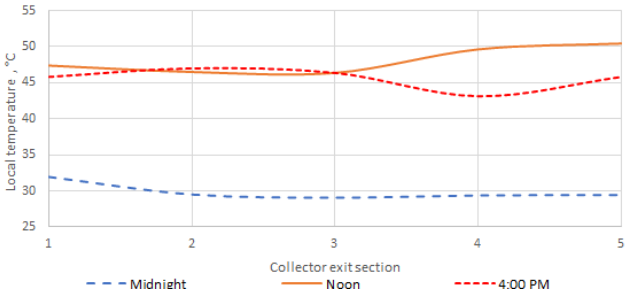

Figure 13. The local temperature at a different time at collector exit

At midnight, the minimum temperature is 29 ^{0}.C. below the collector, and the maximum one is 32 ^{0}.C. at the ground. This switch of maximum temperature between the ground and the roof indeed happens because of the heat storage effect in the ground at night and solar radiation at noon. In other words, a result of direct radiation heat transfer and heat storage in the ground takes place inside the solar chimney collector. At 4:00 PM (middle between noontime and midnight), the temperature below the glass and the ground temperature are the same that reach 45.8 ^{0}C; meanwhile, the temperature at 0.375 m below the collector cover records to be 43 ^{0}.C. The reduction of this temperature may cause by the high local air velocity at this moment.

V. CONCLUSION

Solar chimney power plant (SCPP) produce electricity by combining the solar air heating and chimney effect. The complicated heat transfer process takes place inside the solar chimney collector, ANSYS CFX v18.1 is used to make the 3d simulation of a whole SCPP. To validate the theoretical result, the experimental work is carried out by the SCPP prototype that is implemented in Aswan-Egypt. The local temperature is radially measured at the exit and middle plane of the square collector. The theoretical and experimental results showed a good agreement. The experimental results showed that the energy gains an exchange between the ground and collector roof, depending on the time of solar radiation. This switch of the energy results from switching between direct solar heating and heat storage of the ground. The CFD results present the distribution of velocity and temperature for studying the square and circular shape of collectors. The conclusion that the square collector achieved higher output power than the circular collector by 7.6 % at the same surface area exposed to solar radiation; additionally, the rectangular shape causes a turbulent flow pattern due to change in flow stream lengths that assists in improving the heat transfer process.

VI. ACKNOWLEDGEMENT

This work was supported by the Stipendium Hungaricum Programme and by the Mechanical Engineering Doctoral School, Szent István University, Gödöllő, Hungary.

The solar chimney prototype is part of a joint project funded by the Science and Technology Development Fund (STDF, Project ID 5054) of Egypt and the Federal Ministry of Education and Research (BMBF) of Germany. Also, the turbine blades are donated from Fiber Egypt Company.

VII. REFERENCES

[1] Guo, Penghua, Li, T., Xu, B., Xu, X., & Li, J. (2019). Questions and current understanding about solar chimney power plant: A review. In *Energy Conversion and Management* (Vol. 182, pp. 21–33). Elsevier Ltd. https://doi.org/10.1016/j.enconman.2018.12.063

[2] Muhammed, H. A., & Atrooshi, S. A. (2019). Modeling solar chimney for geometry optimization. *Renewable Energy*, *138*, 212–223. https://doi.org/10.1016/j.renene.2019.01.068

[3] Vieira, R. S., Garcia, C., Junior, I. C. A., Souza, J. A., Rocha, L. A. O., Isoldi, L. A., & Dos Santos, E. D. (2015). Numerical Study of the Influence of Geometric Parameters on the Avaliable Power in a Solar Chimney. *Revista de Engenharia Térmica*, *14*(1), 103. https://doi.org/10.5380/reterm.v14i1.62121

[4] Hassan, A., Ali, M., & Waqas, A. (2018). Numerical investigation on the performance of solar chimney power plant by varying collector slope and chimney diverging angle. *Energy*, *142*, 411–425. https://doi.org/10.1016/j.energy.2017.10.047

[5] Fluri, T. P., & von Backström, T. W. (2008). Comparison of modelling approaches and layouts for solar chimney turbines. *Solar Energy*, *82*(3), 239–246. https://doi.org/10.1016/j.solener.2007.07.006

[6] Gannon, A. J., & Von Backström, T. W. (2002a). Solar chimney turbine part 1 of 2: Design. *International Solar Energy Conference*, 335–341. https://doi.org/10.1115/SED2002-1070

[7] Gannon, A. J., & Von Backström, T. W. (2002b). Solar chimney turbine part 2 of 2: Experimental results. *International Solar Energy Conference*, 343–349. https://doi.org/10.1115/SED2002-1071

[8] Gannon, A. J., & Von Backström, T. W. (2003). Solar chimney turbine performance. *Journal of Solar Energy Engineering, Transactions of the ASME*, *125*(1), 101–106. https://doi.org/10.1115/1.1530195

[9] Jafarifar, N., Behzadi, M. M., & Yaghini, M. (2019). The effect of strong ambient winds on the efficiency of solar updraft power towers A numerical case study for Orkney. *Renewable Energy*, *136*, 937–944. https://doi.org/10.1016/j.renene.2019.01.058

[10] Ming, T., Wang, X., Gui, J., de Richter, R. K., Liu, W., Xu, G., Wu, T., & Pan, Y. (2016). The influence of ambient crosswind on the performance of the solar updraft power plant system. In *Solar Chimney Power Plant Generating Technology* (pp. 163–207). Elsevier. https://doi.org/10.1016/B978-0-12-805370-6.00007-7

[11] Kasaeian, A. B., Heidari, E., & Vatan, S. N. (2011). Experimental investigation of climatic effects on the efficiency of a solar chimney pilot power plant. *Renewable and Sustainable Energy Reviews*, *15*(9), 5202–5206. https://doi.org/10.1016/j.rser.2011.04.019

[12] Zhou, X., Yang, J., Xiao, B., & Hou, G. (2007). Experimental study of temperature field in a solar chimney power setup. *Applied Thermal Engineering*, *27*(11–12), 2044–2050. https://doi.org/10.1016/j.applthermaleng.2006.12.007

[13] Guo, Peng-hua, Li, J., & Wang, Y. (2014). Numerical simulations of solar chimney power plant with radiation model. *Renewable Energy*, *62*, 24–30. https://doi.org/10.1016/j.renene.2013.06.039

[14] Tingzhen, M., Wei, L., Guoling, X., Yanbin, X., Xuhu, G., & Yuan, P. (2008). Numerical simulation of the solar chimney power plant systems coupled with turbine. *Renewable Energy*, *33*(5), 897–905. https://doi.org/10.1016/j.renene.2007.06.021

[15] Mostafa, A. A., Sedrak, M. F., & Dayem, A. M. A. (2011). Performance of a Solar Chimney Under Egyptian Weather Conditions: Numerical Simulation and Experimental Validation. In *Energy Science and Technology* (Vol. 1, Issue 1, pp. 49–63). https://doi.org/10.3968/j.est.1923847920110101.004

[16] Comsan, M. N. H. (2010). SOLAR ENERGY PERSPECTIVES IN EGYPT. *Proceedings of the 4th Environmental Physics Conference*, 1–11. https://www.osti.gov/etdeweb/biblio/21502997

[17] Esmail F.C, M. & Mekhail, T. (2019). Investigations of the instantaneous performance of a solar chimney power plant installed in Aswan using IoT. *IET Renewable Power Generation*, *13*(12), 2261–2266. https://doi.org/10.1049/iet-rpg.2018.5950

[18] Mekhail, T., A-Elmagid, W. M., Esmail F.C, M, Bassily, M., & Harte, R. (2016). Theoretical Investigation of Solar Chimney Power Plant Installed in Aswan City. *International Symposium on Industrial Chimneys and Cooling Towers*.

[19] ANSYS CFX-Solver theory guide. (n.d.). https://www.ansys.com/services/training-center

[20] Krätzig, W. B. (2013). Physics, computer simulation, and optimization of thermo-fluid mechanical processes of solar updraft power plants. *Solar Energy*, *98*, 2–11. https://doi.org/10.1016/j.solener.2013.02.017